

# The Interpolation Method for damage localization in an instrumented steel frame structure



**M.P. Limongelli**

*Politecnico di Milano, Department of Structural Engineering, Milan, Italy*

## **SUMMARY:**

In this paper the recently proposed Interpolation Damage Detecting method (IDDM), a Level 2 damage identification method, is applied to the case of a the Factor Building at UCLA, a densely instrumented building for which responses recorded during several earthquakes are available. The building is a 17-story moment-resisting steel frame structure in the UCLA campus permanently instrumented with an accelerometer array recording both ambient vibrations of the building and motions from local earthquakes. A 3D numerical model of the building has been built calibrating the parameters of the model through the application of an identification procedure to responses recorded during real earthquakes. Several damage scenarios have been simulated for the model and the IDDM has been applied to check its reliability. This application shows that the method allows a reliable detection of the location of damage also for the cases of minor damage patterns.

*Keywords: damage detection, damage location, health monitoring, IDDM, Factor Building*

## **1. INTRODUCTION**

The possibility to timely detect damage in a structure struck by an earthquake can be critical in post-earthquake safety evaluation to establish a hierarchy of both immediate rescue operation and of future strengthening intervention. Traditional methods of damage detection based on visual inspection may be costly, taking a long time to be performed. Experimental techniques, based on magnetic field, thermal field, radiography, ultrasound, etc., allow to obtain detailed information about a local damage state but only if the location of damage is already known. A promising alternative that has received an increasing attention in the last two decades consists in the use of techniques for global damage detection and localization based on the analysis of responses to vibrations recorded on the structures. One of the most important aspects of vibration-based damage detection is the definition of a damage sensitive feature able to reliably assess damage and easily recoverable from recorded responses. A very diffuse approach to this problem is based on the analysis of changes in measured response to vibrations between the undamaged structure and the potentially damaged structure. A comprehensive literature review is reported in Farrar et al (1997) and Sohn et al (2003). In these methods the comparison of the two states is performed in terms of the dynamical characteristics recovered from responses recorded during ambient vibration tests. The difference between the values estimated for the two configurations can be interpreted as a damage function: the extent of damage (if any) is somehow related to the amplitude of the damage function. Some of these methods focus on the changes of modal characteristics: frequencies, mode shapes, modal damping. Several researches however have pointed out that modal parameters alone are not robust estimators of damage being sensitive to errors introduced by the experimental process needed for their evaluation and to environmental changes, to non-linearity in the building response or soil-structure interaction (see Safak, 2005). To overcome these problems, methods that do not need the estimation of modal parameters have been proposed. For example the frequency response curvature method (FRCM) and the Gapped Smoothing Method (GSM) proposed in Sampaio et al.(2001) and Ratcliffe (1997), both define the damage index in terms

of the variation of curvature estimated from operational displacements. The drawback is that the numerical differentiation needed to evaluate curvature introduces errors that often prevent the detection of damage in case of noisy data. The recently proposed Interpolation Damage Detecting method (IDDM) (see Limongelli 2010, 2011) overcomes this drawback through the definition of a damage parameter based on operational displacements rather than curvatures. Basing on the classification system of damage identification methods proposed by Rytter (1993), the method herein presented provides a Level 2 damage identification i.e. it allows to detect and locate damage. The method does not require any finite element modelling of the structure nor requires knowledge of the mechanical and dynamical characteristics of the structure. Furthermore, being based on the mere evaluation of differences between the transfer functions of the recorded signals, it appears feasible to be implemented in a "on line" damage detection warning system that, after a damaging event, can provide, nearly in real time, reliable information about the location of damage that can be critic for post-event intervention.

## 2. THE INTERPOLATION DAMAGE DETECTION METHOD

The idea underlying the proposed method of damage detection can be schematically explained with reference to Figure 1. The two pictures show a snapshot of the deformed shape of two multi-story shear frames undergoing a seismic excitation. The only difference between the two frames is the value of the stiffness of the 5th story columns that, in the frame on the right, is equal to the 80% of the corresponding value in the left frame. Such a reduction of stiffness is assumed to model a damage concentrated at the 5th story.

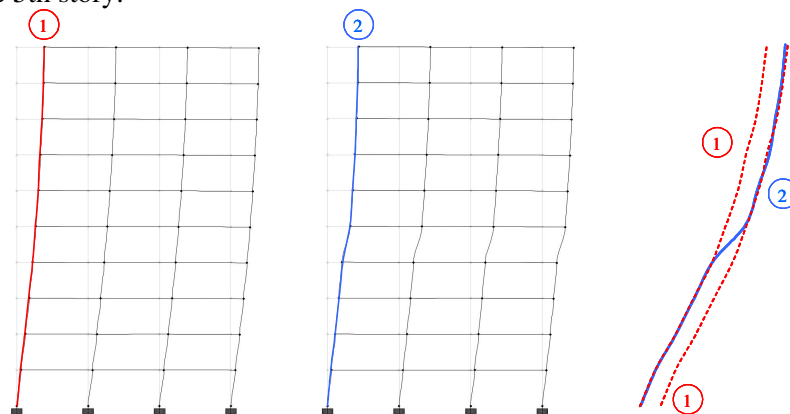


**Figure 1.** Effect of damage

The comparison of the two frames shows that damage causes a sharp variation of the deformed shape occurring at the damaged story. In the stories located below and above the damaged one the two shapes can be almost perfectly superimposed with a simple horizontal shift in the region above the damaged story. A damage detecting feature can thus be defined in terms of the error related to the use of a certain function in modelling the deformed configuration of the structure. Specifically, at a given location of a structure the modelling accuracy could be defined as the difference between the measured displacement and the displacement calculated at that location interpolating through a proper function the displacements measured at all the other locations equipped with a sensor. If the comparison between the interpolation error in two different phases (the baseline phase on the undamaged structure and the inspection phase after a potentially damaging event) shows a significant decrease of accuracy, this is an indication of the existence of damage at a location close to the one where this change has been recorded. In order to remove the influence of the amplitude of displacement on the evaluation of the error function and to remove the errors related to the estimation of displacements from recorded accelerations, the error function has been defined in terms of difference between the transfer functions of the recorded and interpolated accelerations with respect to the input acceleration.

Let  $z_0, z_1, \dots, z_n$ , be instrumented location of the structure where responses in terms of acceleration have been recorded. The frequency response function at each location  $z$  can be calculated interpolating

through a spline shape function the Frequency Response Functions calculated from signals recorded at all the other instrumented locations (the dotted line in Figure 2)

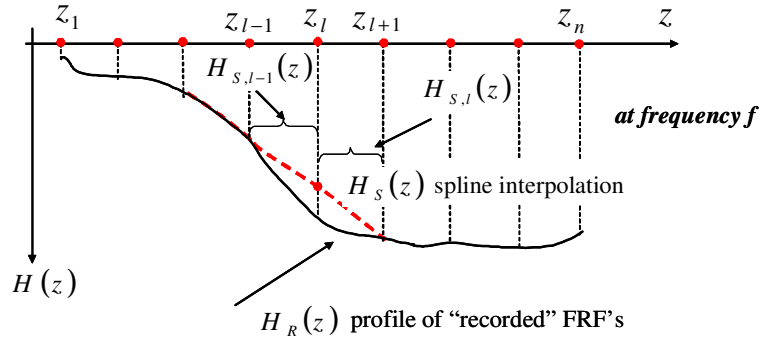


**Figure 2.** Spline interpolation of the FRF at  $z=z_l$ .

At the  $l$ -th location  $z_l$  the FRF can be calculated through the spline interpolation using the following relationship:

$$H_S(z_l, f) = \sum_{j=0}^3 c_{j,l}(f)(z_l - z_{l-1})^j \quad (1)$$

where the coefficients ( $c_{0l}, c_{1l}, c_{2l}, c_{3l}$ ) are calculated from the values of the transfer functions “recorded” at the other locations:

$$c_{j,l}(f_i) = g(H_R(z_k, f_i)) \quad k \neq l \quad (2)$$

In terms of FRF’s the interpolation error at location  $z$  (in the following the index  $l$  will be dropped for clarity of notation) at the  $i$ -th frequency value  $f_i$ , is defined as the difference between the magnitudes of recorded and interpolated frequency response functions:

$$E(z, f_i) = |H_R(z, f_i)| - |H_S(z, f_i)| \quad (3)$$

where  $H_R$  is the FRF of the response recorded at location  $z$  and  $H_S$  is the spline interpolation of the FRF at  $z$ . In order to characterize each location with a single error parameter, the norm of the error on the whole range of frequencies has been considered:

$$E(z) = \sum_{i=1}^N \sqrt{E(z, f_i)^2} \quad (4)$$

$N$  is the number of frequency lines in the Fourier transform correspondent to the frequency range where the signal to noise ratio is high enough to allow a correct definition of the FRF. The values of the frequency response functions depend on the state of the structure hence if the estimation of the error function through equation (4) is repeated in the baseline (undamaged) and in the inspection (potentially damaged) phases, the comparison between the two values, respectively  $E_0$  and  $E_d$  should give an indication about the existence of damage at the considered location.

$$\Delta E(z) = E_d(z) - E_o(z) \quad (5)$$

An increase of the interpolation error between a reference and the current configuration points out a variation of the operational deformed shape hence a variation of stiffness associated with damage. In order to remove the effect of random variations of  $\Delta E$  and assuming a Normal distribution of this function, the 98% percentile is assumed as a minimum value beyond which no damage is considered at that location. In other words a given location is considered close to a damaged portion of the structure if the variation of the interpolation error exceeds the threshold calculated in terms of the mean  $\mu_{\Delta E}$  and variance  $\sigma_{\Delta E}$  of the damage parameter  $\Delta E$  on the population of available records that is:

$$\Delta E(z) > \mu_{\Delta E} + 2\sigma_{\Delta E} \quad (6)$$

The damage index is thus defined as:

$$D(z) = \Delta E(z) - (\mu_{\Delta E} + 2\sigma_{\Delta E}) > 0 \quad (7)$$

### 3. THE FACTOR BUILDING

In this paper the IDDM has been tested using signals recorded on a real building densely instrumented and for which responses recorded during several earthquakes are available. The UCLA Factor building (see Figure 3) is a 17-story moment-resisting steel frame structure consisting of two stories below grade and 15 above grade. The building houses laboratories, faculty offices, administrative offices, the School of Nursing, School of Medicine, auditoriums, and classrooms.

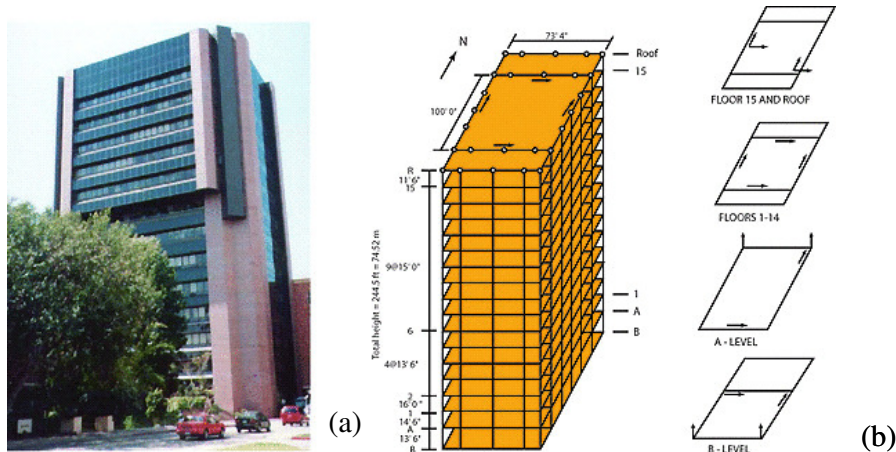


**Figure 3:** The Factor Building (a) East face; (b) Sensors location (from <http://factor.gps.caltech.edu/node/61>)

The building plan is approximately rectangular, longer in the North-South direction and fairly symmetric about the East-West axis. The lateral resisting system is a double bay moment frame with fixed connection between beams and columns. A gravity frame with pinned beams completes the structural scheme. The floors consist of lightweight concrete slab on metal decking. The façade is made of Norman face brick veneer and glass curtain walls supported by an aluminium frame.

The building is permanently instrumented with an embedded 72-channel accelerometer array recording both ambient vibrations of the building and motions from local earthquakes. The sensors array is composed by four horizontal channels per floor: two in North-South direction and two in East-West direction. The two floors below grade are also equipped with two vertical channels. The array continuously records ambient vibrations as well as motions from local earthquakes. More details on the Factor Building and on the recording network can be found in Kohler et al (2005) and Skolnik et al (2006) and <http://factor.gps.caltech.edu/node/61> (last accessed April 2012).

#### The “Reference signature”

As previously mentioned, the damage detection is performed comparing the values of the interpolation error function  $E_d$  in the (possibly) damaged configuration to the values  $E_o$  of the function in the initial (undamaged) configuration of the building. This latter is assumed as a reference state of the structure. Deviations from the reference state point out the occurrence of changes (damages) in the configuration of the building. The first step in the application of the damage detection procedure is the calculation of  $E_o$  that is a sort of “signature” of the structure in the initial configuration. For the Factor building the availability of responses recorded during several local and regional earthquakes allows the evaluation of the original function  $E_o$ .

The network of sensors deployed on the Factor building records responses in two directions as showed in Figure 3b: at each floor 4 responses are recorded, two in North directions located in the East (NE) and in the West (NW) part of the building and 2 in the East direction in the North (EN) and in the South (ES) part of the building.

Assuming a rigid diaphragm behaviour of each floor, the components of the absolute accelerations at the reference point shown in Figure 4 are calculated and assumed as the story absolute accelerations. The following relations were used to calculate floor accelerations:

$$\ddot{\theta}_R = \frac{1}{2} \left[ \frac{(\ddot{u}_2 - \ddot{u}_1)}{(y_1 + y_2)} + \frac{(\ddot{v}_2 - \ddot{v}_1)}{(x_1 + x_2)} \right]$$

$$\ddot{u}_R = \ddot{u}_1 + \ddot{\theta}_R y_1$$

$$\ddot{v}_R = \ddot{v}_1 + \ddot{\theta}_R x_1$$

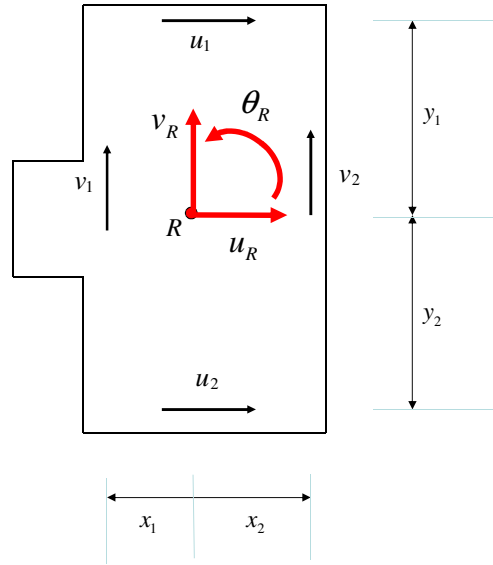


**Figure 4:** Floor plan. Sensors location and reference point

For each direction  $x$  and  $y$  of the building the signature of the building can be calculated using responses in that direction at the reference point of each storey. The frequency response functions (FRF)  $H_{R_x}$  and  $H_{R_y}$  of absolute acceleration in  $x$  and  $y$  directions have been calculated, each with respect to the component of the base input in the same direction. Hence  $H_{R_x}$  is the frequency response function of the absolute acceleration along  $x$  with respect to the  $x$  component of the base excitation;  $H_{R_y}$  is the frequency response function of the absolute acceleration along  $y$  with respect to the  $y$  component of the base excitation.

The values of the interpolation errors  $E_{ox}$  and  $E_{oy}$  in the two directions have thus been calculated using equation (4). For each of the two directions, the reference signature has been determined using the responses of the model to a number of base inputs chosen between the several dozens of small to intermediate local and regional earthquakes that have been recorded at the base of the Factor Building. Table 1 reports the characteristics of these earthquakes: date of occurrence, peak acceleration of the ground motion  $a_g$ , magnitude  $ML$  and distance from the epicentre  $\Delta$ .

The ground shaking for all these events is small enough to assume a linear behaviour of the building and neglect nonlinear effects. For each event the responses at each storey of the model have been used to calculate the interpolation errors in  $x$  and  $y$  directions at that storey.

**Table 1. Characteristics of the input motions**

	Earthquake date	$a_{max}$ ( $g$ ) $\times 10^{-3}$	$ML$	$\Delta$ ( $km$ )
1	2005_Feb 27	1.15	2.9	9
2	2005_Mar 23	1.21	3.4	20.6
3	2005_Apr 16	1.12	5.2	126.1
4	2005_Apr 29	0.88	2.8	8.7
5	2005_Jun 12	1.85	5.2	183.1
6	2005_Jun 23	0.28	2.8	9.7
7	2005_Sep 22	0.66	4.7	120.4
8	2005_Oct 16	0.48	4.9	180.6
9	2005_Oct 22	2.02	3.1	7.1
10	2005_Oct 23	2.28	3.1	6.6

In each of the two directions  $x$  and  $y$ , the mean value of the interpolation error calculated for all the events, has been assumed as the reference signature. These base inputs, each 30000 points long (about

5 minutes at 100Hz sampling) were down sampled at 50Hz in order to remove high frequency noise and to reduce the size of data having, at the same time, a cut-off frequency greater than the maximum modal frequency of the frame.

Figure 5 shows function  $E_{ox}$  calculated from responses recorded during ten different small earthquakes that stroke the Factor Building in 2004. The figure shows that the values of the function calculated for several earthquakes exhibit very low variations at each location confirming the assumption of the independence of this function from the base input.

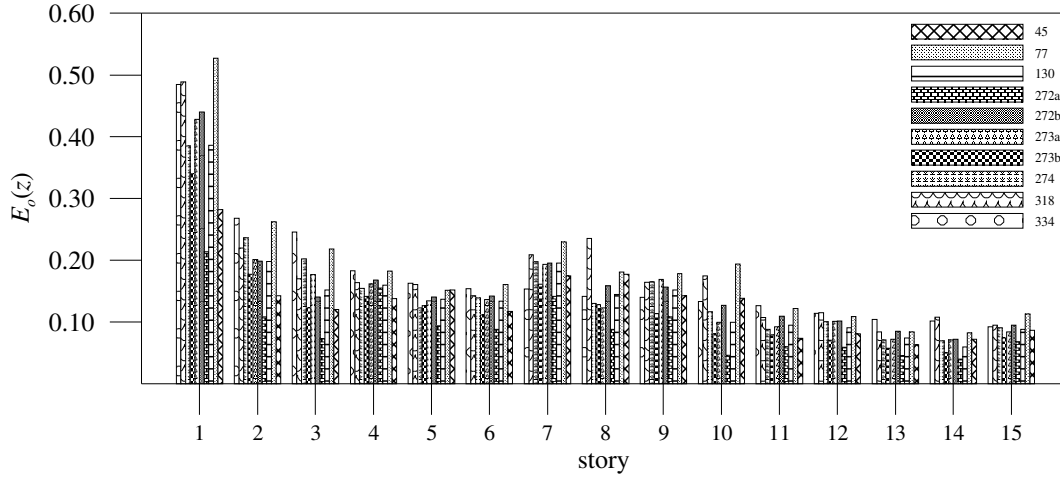


**Figure 5:** Reference signature: error function for 10 earthquakes recorded on the Factor Building

### The finite elements model

At the time being only responses recorded during non-damaging events are available for the Factor Building hence it is not possible to test the performance of the IDDM in damage detection using recorded responses. To this aim a numerical model of the building has been developed on the base of structural drawing and calibrated using the results of an identification procedure to data recorded during Parkfield earthquake of 28 September 2004. The finite element model has been built using as a starting point the model used in reference Skolnik et al.(2006). The main differences between the original model and the one used for this work, concerns the modelling of non-structural elements and of storey masses. Brick veneer (BV) and Glass Curtain Walls (GCV) on the building façades, are modelled herein as shell elements with the characteristics reported in Table 2.

**Table 2. Characteristics of the exterior wall system**

	Brick Veneer	Glass Curtain Walls
Thickness (cm)	3.8	0.64
Weight density (kN/m <sup>3</sup> )	32	38
Elastic Moduli (MPa)	2500	4350

The values of thickness and density are recovered from Skolnik et al.(2006) while the elastic moduli of materials have been chosen in a range of values reasonable for the material in order to match the identified modal parameters Floors are modelled as rigid diaphragm where in-plane relative displacements are prevented. The weight density of the floors has been assumed equal to 20kN/m<sup>3</sup> for storeys 1 to 8 and equal to 30kN/m<sup>3</sup> for storeys 9 to 15. This distribution of masses together with the introduction in the model of the stiffness of non-structural elements allows a close match between calculated and identified modal properties.

The modal analysis of this numerical model found for the first 9 modal frequencies of the structures the values reported in Table 3. The table also reports the values of the modal parameters identified by different research groups from responses recorded during several different small California earthquakes: 3 September 2002 Yorba Linda, 28 March 2003 Encino, 28 September 2004 Parkfield. The comparison between the values identified and calculated from the model shows that there is a very good match for the first 8 frequencies with maximum error lower than 5% for the Parkfield results.

The error reaches 20% for the 3<sup>rd</sup> torsional mode. This is probably due to the simplified distribution of floor masses adopted for the model but this approximation was considered acceptable for the model due to its scarce influence on the results of the damage detection procedure herein presented.

**Table 3. Modal frequencies identified and calculated from the model**

Modo	Yorba Linda. 0 (from Kohler et al 2005)	Encino (from Kohler et al 2005)	Parkfield (from Skolnik et al 2006)	F.E. Model.
1° E-W	0.51	0.50	0.47	0.47
1° N-S	0.57	0.52	0.50	0.50
1°tors.	0.70	0.70	0.68	0.70
2° E-W	1.45-1.55	1.40÷1.65	1.49	1.48
2° N-S	1.60÷1.75	1.50÷1.80	1.66	1.63
2°tors.	/	/	2.36	2.33
3° E-W	2.65÷2.85	2.45÷2.80	2.68	2.59
3° N-S	2.75÷3.10	2.70÷3.05	2.86	2.73
3°tors.	/	/	3.82	3.03

### Damage scenarios

Different damage scenarios have been simulated considering damage to:

- 1) glass curtain walls of the façade (GCW);
- 2) brick veneer (BV);
- 3) columns of one or more storeys of one or more frames in  $x$  and  $y$  directions;
- 4) several combinations of scenarios 1 to 3.

Damage to the glass curtain walls and to the brick veneer has been simulated by reducing the elastic moduli of the materials; damage to columns is modelled by applying moment releases at their end connections.

### Noise in recorded data

In order to study its influence on the reliability of the method, noise has been added to responses. Noise has been modelled as a Gaussian zero mean white noise vector: several different simulations were carried out considering values of noise increasing from 0.1% to 5. The percentages represent the ratio between the root mean square of added noise and the root mean square of the amplitude of the absolute acceleration.

## 4. RESULTS

Results for the different damage scenarios are reported in the following figures. The actual damage location is shown by the red vertical bar.

Scenarios of type 2, characterized by damage at the brick veneer only, cannot be reliably identified by the method hence results are not reported herein. On the contrary for scenarios with damage at glass curtain walls or columns (type 1, 3, and 4) the method allows an accurate localization of damage even when noise affects recorded signals.

For scenarios with damage at one single interstory (Figure 6) results obtained from responses in the same direction of the damaged frame are reported. The analysis of responses in the orthogonal direction does not allow any detection and localization of damage. The comparison between results obtained by considering responses in both directions  $x$  and  $y$  allows to correctly localize the direction ( $x$  or  $y$ ) of the damaged frame and the position of damage (interstory 7-8). At the increase of damage that is at the increase in the number of the damaged elements also the damage index  $D(z)$  increases.

Namely  $D(z)$  in both directions  $x$  and  $y$  is lower for damage only to the glass curtain walls ( $g$ ), higher for damage only to the columns ( $c$ ) and reaches the maximum values for damage to both the glass curtain walls and the columns ( $gc$ ). Also for the case of damage to frames in both directions  $x$  and  $y$  (Figure 7) the position of damage is correctly detected. Using responses in one direction ( $x$  or  $y$ ) it is possible to detect damage only to frames in the same direction. For example for scenario  $D_{x7-8\_y1\_2}$

responses in the  $x$ -direction (dashed line) allow to detect just damage at story 7 while responses in the  $y$ -direction detect just damage at story 1. For the case of scenario  $D_{x1-2\_y1\_2}$  responses in both directions correctly detect damage at story 1.

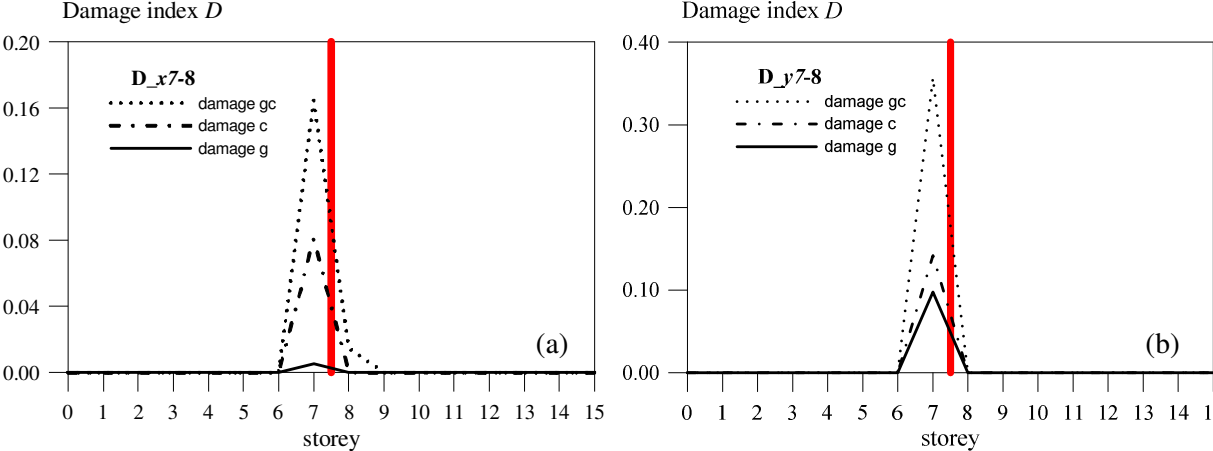


**Figure 6.** (a) Damage to the frame in the  $x$  direction at the interstorey 7-8; (b) Damage to the frame in the  $y$  direction at the interstorey 7-8

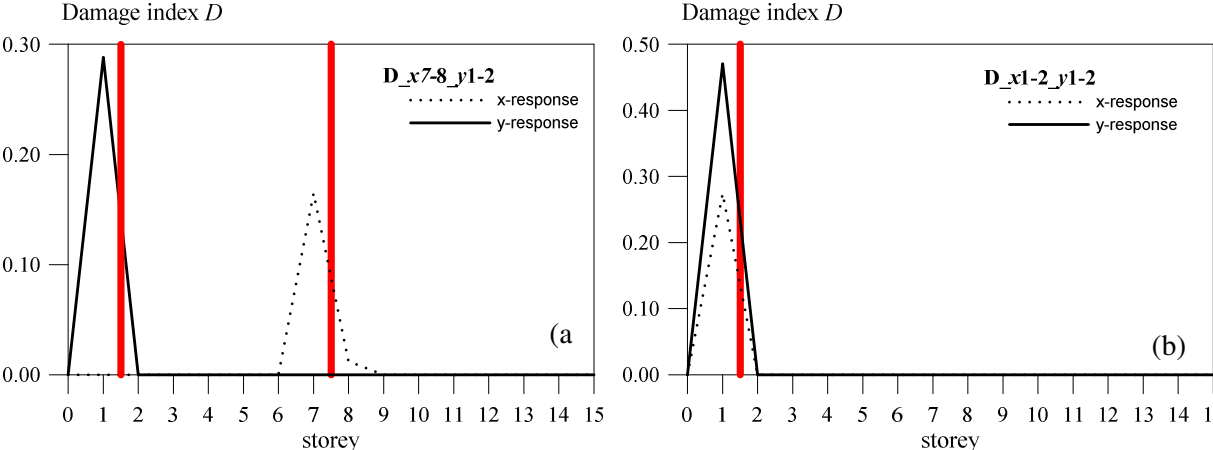


**Figure 7.** (a) Damage to the frame in the  $x$  direction at the interstorey 7-8 and in the  $y$ -direction at the interstorey 1-2; (b) Damage to the frame in the  $x$  direction and in the  $y$  direction at the interstorey 1-2

**Influence of noise on results**

The accuracy of results given by the method depends on the damage level and on the level of noise. For a given intensity of noise the reliability of the method decreases at the increase of noise in recorded data. Results reported in the previous section have been obtained assuming 0.1% noise to signal ratio (in terms of RMS of recorded signal) that is a very low level of noise. Figure 8 to Figure 10 report, for values of noise to signal ratio increasing from 0.1% to 5%, results relevant to scenarios of type 4 that is with damage to both columns and glass curtain walls in just one direction. At the increase of noise in recorded data the value of the damage index decreases but in all the considered cases the position of the damaged section is correctly detected.



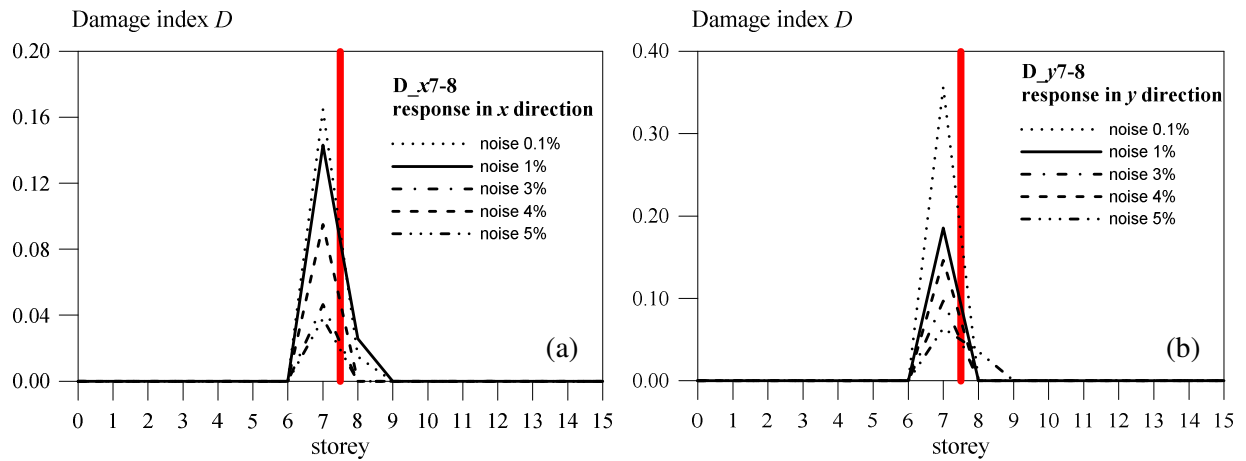


**Figure 8.** (a) Damage to a frame in the  $x$  direction at the interstorey 7-8 for different levels of noise (b) Damage to a frame in the  $y$  direction at the interstorey 7-8 for different levels of noise

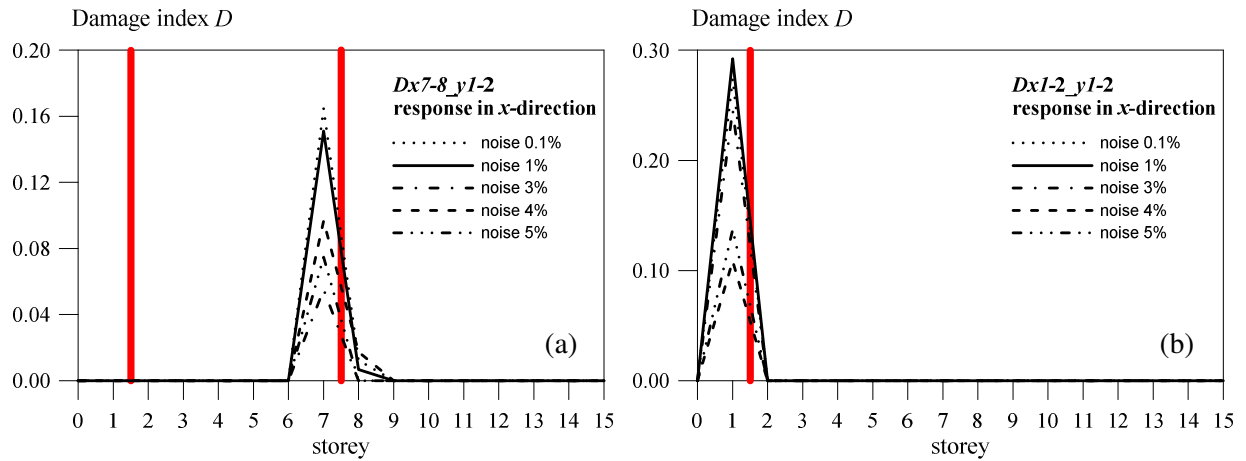


**Figure 9.** (a) Damage in the  $x$  and  $y$  directions detected using responses in the  $x$  direction

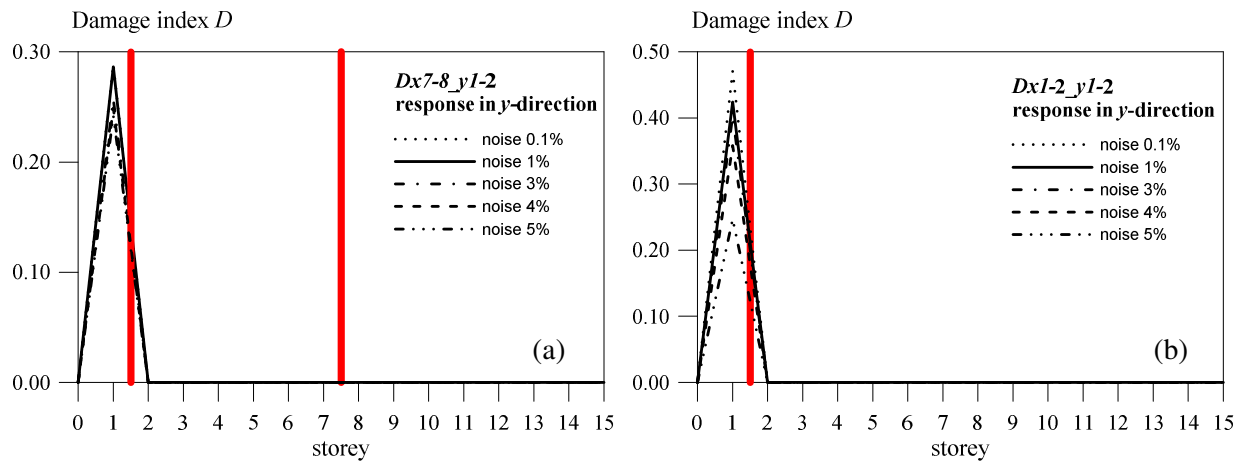


**Figure 10.** (a) Damage in the  $x$  and  $y$  directions detected using responses in the  $y$  direction

Figure 9 and Figure 10 report results relevant to two scenarios of type 4 that is with damage to both columns and glass curtain walls in both directions. Results have been obtained by considering separately the responses in  $x$  and  $y$  directions. Also in this case the damage index decreases at the increase of noise in recorded data but the location of the damaged section is always correctly detected together with the direction of the frame to which the damaged elements belong.

Using only responses in the  $x$  direction the method gives the indication that damage is located at the interstory 7-8 (Figure 9a) or only at the interstory 1-2 (Figure 9b). If the responses in the  $y$  direction are used the method denounces damage only at the interstory 1-2 in both cases (Figure 10a and Figure 10b). This means that using responses in both directions the IDDM allows to correctly detecting the position and the direction of the damaged element.

## CONCLUSIONS

The Interpolation Damage detection Method has been applied to the case of a real densely instrumented multi-storey steel building ad UCLA. A calibrated numerical model of the building has been used to simulate several damage scenarios. Results show that, even for the case of noisy data, this method allows a reliable detection of the location of damage provided a sufficiently dense network of instruments is deployed. This is particularly important for the case of minor damage patterns where traditional methods based, for example, on visual inspection are unable to both detect and locate damage. The main advantage of the IDDM with respect to other methods of damage detection is that it does not require a numerical model of the structure as well as an intense data post-processing or user interaction. For these reasons this method appears as a valid option for automated damage assessment, able to provide after a damaging event, reliable information about the location of damage.

## ACKNOWLEDGMENTS

The author wish to thank the USGS ANSS program and the NSF Center for Embedded Networked Sensing at UCLA for the availability of data recorded on the factor Building and dr. Derek Skolnik for the availability of his numerical model of the Factor Building.

## REFERENCES

- Farrar, C. R. and Doebling, S. W., (1997). "An Overview of Modal-Based Damage Identification Methods," *EUROMECH 365 International Workshop: DAMAS 97, Structural Damage Assessment Using Advanced Signal Processing Procedures*, Sheffield, U.K.
- Kohler, M. D., P. M. Davis, and E. Safak, (2005). Earthquake and ambient vibration monitoring of the steel-frame UCLA Factor building, *Earthquake Spectra*, 21, 715-736.
- Limongelli M.P. (2010). "Frequency response function interpolation for damage detection under changing environment". MSSP doi:10.1016/j.ymsp.2010.03.004
- Limongelli, M.P., (2011). The interpolation damage detection method for frames under seismic excitation. *Journal of Sound and Vibration*, 330. 5474–5489.
- Sampaio R.P.C., Maia N.M.M., Silva J.M.M. (1999) "Damage detection using the frequency response function curvature method". *Journal of Sound and Vibration* 226(5) 1029-1042.
- Ratcliffe C.P. (1997) "Damage Detection Using A Modified Laplacian Operator On Mode Shape Data". *Journal of Sound and Vibration* 204(3) 505 517.
- Rytter A., (1993) "Vibration based inspection of civil engineering structures," *Ph. D. Dissertation, Department of Building Technology and Structural Engineering*, AalborgUniversity, Denmark.
- Safak, E. (2005). Detection of seismic damage in structures from continuous vibration records (invited paper), *Proceedings, 9th International Conference on Structural Safety and Reliability (ICOSSAR)*, Rome, Italy, June 19-23 2005.
- Sohn, H., Farrar, C. R., Hemez, F. M., Shunk, D. D., Stinemates, D. W., and Nadler, B. R. (2003). "A review of structural health monitoring literature: 1996-2001." *Rep. No. LA-13976-MS, Los Alamos National Laboratory*, Los Alamos, N.M.
- Skolnik, D.; Ying, L.; Yu, E.; and Wallace, J. W., (2006) "Identification, Model Updating, and Response Prediction of an Instrumented 15-Story Steel Frame Building," *Earthquake Spectra*, vol. 22, no. 3 781-802.